Journal of Mathematical Modeling
Vol. 14, No. 1, 2026, pp. 19-34. Research Article

JMM

An accurate computational approach for solving system of differential equations involving non-local derivatives

Gaurav Saini [†], Bappa Ghosh [‡*], Sunita Chand [§]

[†] *Center for Data Science, Department of Computer Science and Engineering, Siksha 'O' Anusandhan (Deemed to be University),* INDIA
[‡] *Center for Artificial Intelligence and Machine Learning, Department of Computer Science and Engineering, Siksha 'O' Anusandhan (Deemed to be University),* INDIA
[§] *Department of Mathematics, Siksha 'O' Anusandhan (Deemed to be University),* INDIA.

Email(s): gauravsaini@soa.ac.in, bg12.ghosh@gmail.com, sunitachand@soa.ac.in

Abstract. This paper addresses the numerical approximation of a system of differential equations involving fractional derivatives of arbitrary order. The derivatives are governed in the Caputo sense of orders $\alpha_i \in (0,1)$. Motivated by the complexity of modeling coupled fractional dynamics, an efficient numerical scheme based on the classical L1 discretization technique is developed. The proposed method effectively captures the behavior of the system across various fractional orders and parameter regimes. A rigorous convergence analysis confirms the consistency of the proposed technique and establishes a convergence rate of order $\min_p\{2-\alpha_p\}$. Numerical experiments are conducted to validate the theoretical findings, demonstrating excellent agreement with exact solutions and confirming the computational efficiency of the approach. These results highlight the robustness of the proposed scheme for solving the differential system with memory effects.

Keywords: System of differential equations, Caputo derivative, L1 scheme, convergence analysis.
AMS Subject Classification 2010: 26A33, 34A30, 65L05.

1 Introduction

Fractional calculus is a generalization of classical calculus that extends the concept of derivatives and integrals to non-integer (fractional) orders. This field has gained significant attention due to its ability to model memory and hereditary properties inherent in various physical and biological systems. Unlike integer-order models, fractional-order models can better capture long-range temporal or spatial interactions, making them ideal for processes with non-local effects. Applications of fractional calculus are

*Corresponding author
Received: 01 June 2025 / Revised: 21 August 2025 / Accepted: 21 August 2025
DOI: 10.22124/jmm.2025.30849.2765

found in diverse fields such as viscoelasticity, control theory, signal processing, diffusion processes, bioengineering, etc [10, 11, 14, 21, 23]. The two most commonly used definitions of fractional derivatives are the Caputo and Riemann–Liouville derivatives, each suited for different types of problems. In many physical and engineering problems, initial conditions are naturally given in terms of integer-order derivatives (e.g., initial position, velocity). Caputo derivative allows these classical initial conditions to be applied directly, making the modeling process more intuitive and physically meaningful. In contrast, the Riemann–Liouville derivative requires initial conditions defined via fractional derivatives, which are often difficult to interpret physically and to implement in practice. This makes the Caputo derivative better suited for describing processes. Systems of ordinary differential equations (ODEs) arise when modeling real-world phenomena involving multiple interdependent variables that change with respect to a common independent variable, typically time or space. These systems are central in fields such as population dynamics, electrical circuits, chemical reactions, and mechanical systems. Depending on the nature of the equations, ODE systems can be linear or nonlinear, autonomous or non-autonomous . If the order of differential equations is non-local, the system transitions into the domain of fractional differential equations (FDEs). These equations offer a more accurate description of processes exhibiting memory effects and hereditary properties compared to traditional integer-order ODEs. The application of fractional calculus in these contexts provides deeper insights into systems with irregular or complex behaviors, yielding more precise results. In general, due to the unavailability of exact analytical solutions, researchers across various fields focus on developing efficient numerical techniques for solving FDEs while ensuring their stability and convergence. The Morris-Lecar model, originally proposed in 1981, is a reduced biophysical model that describes the membrane potential dynamics of excitable cells, such as neurons and muscle fibers. It simplifies the more complex Hodgkin-Huxley model by reducing it to a two-dimensional system, capturing essential features of neuronal excitability with lower computational complexity. The model is particularly effective in analyzing neuronal firing patterns, type-I and type-II excitability, and oscillatory behaviors near bifurcation points. The classical form of the Morris–Lecar model consists a pair of coupled ODEs given by

$$\begin{cases} C\frac{dV}{dt} = I_{\text{app}} - g_{\text{L}}(V - V_{\text{L}}) - g_{\text{Ca}}M_{\infty}(V)(V - V_{\text{Ca}}) - g_{\text{K}}N(V - V_{\text{K}}), \\ \frac{dN}{dt} = \frac{N_{\infty}(V) - N}{\tau_N(V)}, \end{cases} \tag{1}$$

where V is the membrane potential, N is the recovery variable, and the other parameters represent ionic conductances and reversal potentials. $M_{\infty}(V)$ and $N_{\infty}(V)$ are voltage-dependent activation functions, while $\tau_N(V)$ is a time constant. Recent research has extended the Morris-Lecar model to incorporate fractional-order derivatives, motivated by the need to capture memory and hereditary effects observed in neuronal dynamics. These extensions replace the classical derivatives of (1) by the derivatives of non-integer order as follows

$$\begin{cases} C\mathscr{D}_t^{\alpha_1}V(t) = I_{\text{app}} - g_{\text{L}}(V - V_{\text{L}}) - g_{\text{Ca}}M_{\infty}(V)(V - V_{\text{Ca}}) - g_{\text{K}}N(V - V_{\text{K}}), \\ \mathscr{D}_t^{\alpha_2}N(t) = \varphi\ell(V)(N_{\infty}(V) - N), \end{cases}$$

where $\mathscr{D}^{\alpha_i}$ denotes the Caputo derivative of order $\alpha_i \in (0,1)$, with $\alpha_1 \neq \alpha_2$ in the incommensurate case. Such models provide a richer and more accurate framework for analyzing subdiffusive and long-term memory behavior in neuronal systems. Upon linearization around an equilibrium point, the fractional Morris–Lecar system reduces to a linear inhomogeneous system of the form:

$$\mathscr{D}_t^{\alpha}\mathbf{U}(t) + \mathbf{A}(t)\mathbf{U}(t) = \mathbf{F}(t),$$

which corresponds directly to the type of multi-order fractional system considered in this work. This connection highlights the practical relevance of our system in modeling real-world dynamical processes in neurophysiology that involve memory and complex coupled behavior.

In this article, we consider the following general class of fractional-order systems

$$\begin{cases} \mathscr{D}_t^{\alpha}\mathbf{V}(t)+\mathbf{A}(t)\mathbf{V}(t)=\mathbf{F}(t), \quad t\in(0,T], \\ \mathbf{V}(0)=\mathbf{V}_0, \end{cases} \tag{2}$$

where $T\in\mathbb{R}^+$, $\mathbf{V}$ is the unknown vector function which is required to be evaluated and

$$\begin{cases} \alpha=[\alpha_1,\alpha_2,\ldots,\alpha_n], \;\; \mathbf{A}(t)=[a_{ij}(t)],\; i,j=1,2,\ldots,n, \\ \mathbf{V}(t)=[v^{(1)}(t),v^{(2)}(t),\ldots,v^{(n)}(t)]^T, \\ \mathbf{F}(t)=[f^{(1)}(t),f^{(2)}(t),\ldots,f^{(n)}(t)]^T, \\ \mathbf{V}_0=[v^{(1)}(0),v^{(2)}(0),\ldots,v^{(n)}(0)]^T, \end{cases}$$

where $\alpha_i\in(0,1)$ for each i, $a_{ij}:[0,T]\to\mathbb{R}$, and the vector function $\mathbf{F}(t)$ are known and sufficiently smooth. The theoretical and numerical analysis of FDEs poses significant challenges, primarily due to the nonlocal nature of fractional derivatives. This nonlocality complicates the derivation of exact analytical solutions for most real-world problems, thereby motivating the development of robust and efficient numerical methods. Several numerical approaches have been proposed in the literature for fractional systems, including finite difference, finite element, and spectral methods. The existence and uniqueness of solutions for initial value problems involving fractional-order systems have been rigorously studied in foundational works such as those by Delbosco and Rodino [4], and later by Odibat [17], who provided generalizations under various fractional operators. In [8] Khader *et al.* introduced the Chebyshev collocation method for solving high-order FDEs, demonstrating its ability to yield accurate approximations for complex systems. Chen *et al.* [3] developed a multi-domain spectral method for time-FDEs, combining three-term recurrence relations for Jacobi polynomials with high-order Gauss quadrature. Their approach achieved high-order accuracy across domain partitions. In [6] Duan *et al.* presented two spectral approximation strategies-one based on truncated series expansion and the other on interpolation using shifted Jacobi polynomials—to approximate the fractional derivative. Coupled with a collocation method, both techniques provided highly accurate solutions with provable exponential convergence for smooth problems. Diethelm *et al.* [5] examined the asymptotic behavior of linear multi-order fractional systems, offering a theoretical framework that supports stability analysis and long-term solution behavior-key aspects for reliable numerical modeling. Ziane and Cherif [25] proposed the Variational Iteration Transform Method, a hybrid technique that combines the Variational Iteration Method with the Laplace transform to solve linear and nonlinear FDEs. In [22] Soradi-Zeid developed direct and indirect meshless methods based on radial basis functions to solve fractional optimal control problems. These methods approximated both the state and control variables without requiring meshing, and yielded precise results for multi-dimensional fractional systems. In the same year, Ruman *et al.* [19] applied the Galerkin method to linear fractional-order two-point boundary value problems, addressing both homogeneous and nonhomogeneous cases. Their approach utilized differentiable polynomial basis functions. Abdeljawad *et al.* in [1], introduced a Haar wavelet collocation technique to solve systems of FDEs. By expanding unknown functions in Haar series and using collocation points, they transformed the system

into algebraic equations and demonstrated significant computational savings. Most recently, Algazaa and Saeidian [2] presented two powerful numerical strategies for nonlinear multi-order fractional systems. The first one employed a fractional operational matrix based on Bernstein polynomials, while the second one utilized a spectral collocation method with Bernstein polynomials at Chebyshev–Gauss–Lobatto points, evaluated through Jacobi–Gauss quadrature. Recent advances in numerical treatment of fractional systems can be found in [9,12,16,20,24], where efficient iterative and spectral methods have been proposed.

These diverse methodologies demonstrate the rapid evolution of numerical techniques for solving FDEs. They provide a solid foundation for further exploration into stable and accurate schemes, particularly for multi-variable, multi-order systems like those considered in this study. While earlier work have addressed numerical methods for scalar or linear multi-term fractional differential equations, they do not fully explore systems with multiple Caputo fractional derivatives of distinct orders, especially in a coupled nonlinear setting. In contrast, the present work develops and analyzes a generalized L1 scheme tailored for such systems, offering both theoretical convergence guarantees and numerical validation. The L1 scheme is used to approximate the fractional derivative of order $\alpha \in (0,1)$. It is derived using a piecewise linear interpolation of the integrand over each subinterval. Owing to its simple form and ease of implementation, the L1 approximation has been widely employed in the numerical treatment of both single and multi-term fractional differential equations; see [7,13,15,20] and the references therein. However, fewer studies have explored its implementation in coupled systems involving multiple Caputo fractional orders with distinct dynamics. The novelty of our proposed scheme lies in its tailored adaptation of the classical L1 method to a multi-dimensional setting, allowing for component-wise treatment of distinct fractional orders.

The main objective of this study is to develop and analyze a robust and accurate numerical method based on the classical L1 difference scheme for solving systems of differential equations involving fractional derivatives. The method is designed to handle multi-order coupled systems and to effectively capture the non-local memory effects characteristic of such systems. By leveraging the structure of the Caputo derivative, the approach ensures compatibility with classical initial conditions and offers provable convergence behavior, as validated through both theoretical analysis and numerical experiments. The structure of the paper is as follows In Section 2, we present fundamental definitions from fractional calculus. The construction of the numerical scheme for solving (2) is provided in Section 3. The convergence analysis is done in Section 4. Section 5 focuses on numerical simulations, and concluding remarks are presented in Section 6.

2 Preliminaries

The following definitions and properties will be useful for this work. For more detail one may refer [18].

Definition 1. *Let $\phi(t) \in \mathscr{C}[a,b]$, the Riemann-Liouville fractional integral of order $\nu \in \mathbb{R}^+$ of $\phi(t)$ is defined by*

$$J_t^{\nu}\phi(t) = \frac{1}{\Gamma(\nu)} \int_a^x (x-t)^{\nu-1}\phi(t)\,dt,$$

$\Gamma(\cdot)$ is Euler's gamma function.

Definition 2. *Let $n-1<\nu\leq n, n\in\mathbb{N}$. The Caputo derivative of order $\nu\in\mathbb{R}^+$ of the function $\phi(t)\in\mathscr{C}^n[a,b]$, is defined by*

$$\mathscr{D}_t^{\nu}\phi(t)=\begin{cases}\dfrac{1}{\Gamma(n-\nu)}\displaystyle\int_a^x(x-t)^{n-\nu-1}\phi^{(n)}(t)\,dt & \text{if} \quad n-1<\nu<n,\\ \phi^{(n)}(t) & \text{if} \quad \nu=n.\end{cases}$$

Definition 3. *The two parameters $\beta,\gamma>0$ Mittag-Leffler function is defined by*

$$E_{\beta,\gamma}(z)=\sum_{k=0}^{\infty}\frac{z^k}{\Gamma(\beta k+\gamma)},\qquad z\in\mathbb{C}.$$

The following are some basic properties of the fractional calculus:

- Linearity: Let λ_1,λ_2, be positive constants, then

$$J_x^{\nu}\{\lambda_1\varphi_1(t)\pm\lambda_2\varphi_2(t)\}=\lambda_1 J_x^{\nu}\varphi_1(t)\pm\lambda_2 J_x^{\nu}\varphi_2(t),$$
$$\mathscr{D}_x^{\nu}\{\lambda_1\varphi_1(t)\pm\lambda_2\varphi_2(t)\}=\lambda_1\mathscr{D}_x^{\nu}\varphi_1(t)\pm\lambda_2\mathscr{D}_x^{\nu}\varphi_2(t).$$

- For $x\in[a,b]$, $m-1<\nu<m$, we have

$$\mathscr{D}_x^{\nu}J_x^{\nu}\varphi(t)=\varphi(t)\quad\text{and}\quad J_x^{\nu}\mathscr{D}_x^{\nu}\varphi(t)=\varphi(t)-\sum_{k=0}^{n-1}\varphi^{(k)}(a^+)\frac{(x-a)^k}{k!},\ \ x>a.$$

3 The discretized problem

Let $N\in\mathbb{N}$. The uniform mesh $t_j=j\tau$ for $j=0(1)N$ with equal step length $\tau=T/N$. The computed solution of $v^{(p)}$ at the mesh point t_j is denoted by $V_j^{(p)}$. $\mathscr{D}_t^{\alpha_p}v^{(p)}(t)$ at t_j for $j=1(1)N$ can be written as

$$\mathscr{D}_t^{\alpha_p}v^{(p)}(t_j)=\frac{1}{\Gamma(1-\alpha_p)}\sum_{k=0}^{j-1}\int_{s=t_k}^{t_{k+1}}(t_j-s)^{-\alpha_p}\,(v^{(p)}(s))'\,ds,$$

for $p=1(1)n$, which can be discretized as follows [13]:

$$\begin{aligned}\mathscr{D}_N^{\alpha_p}v^{(p)}(t_j)&=\frac{1}{\Gamma(1-\alpha_p)}\sum_{k=0}^{j-1}\frac{v^{(p)}(t_{k+1})-v^{(p)}(t_k)}{\tau}\int_{s=t_k}^{t_{k+1}}(t_j-s)^{-\alpha_p}\,ds\\&=\frac{\tau^{-\alpha_p}}{\Gamma(2-\alpha_p)}\sum_{k=0}^{j-1}\left[v^{(p)}(t_{k+1})-v^{(p)}(t_k)\right]b_{j-k}^{(p)},\end{aligned}\tag{3}$$

with the truncation error $\varepsilon_j^{(p)}=(\mathscr{D}_t^{\alpha_p}-\mathscr{D}_N^{\alpha_p})\,v^{(p)}(t_j)$ and the coefficient $b_q^{(p)}=q^{1-\alpha_p}-(q-1)^{1-\alpha_p}$ for $q=1(1)N$. Using (3), model (2) is transformed to

$$\begin{cases}\mathscr{D}_N^{\alpha_p}v^{(p)}(t_j)+\displaystyle\sum_{i=1}^{n}a_{pi}(t_j)\,v^{(i)}(t_j)=f^{(p)}(t_j)+\varepsilon_j^{(p)},\quad j=1(1)N,\\ v^{(p)}(t_0)=\eta_p,\end{cases}\tag{4}$$

for each $p = 1(1)n$. Neglecting the remainder term $\varepsilon_j^{(p)}$, the discrete problem (4) reduces to

$$\begin{cases} \dfrac{\tau^{-\alpha_p}}{\Gamma(2-\alpha_p)} \displaystyle\sum_{k=0}^{j-1} \left(V_{k+1}^{(p)} - V_k^{(p)}\right) d_{j-k}^{(p)} + \sum_{i=1}^{n} (a_{pi})(t_j) V_j^{(i)} = f_j^{(p)}, \quad j = 1(1)N, \\ V_0^{(p)} = \eta_p, \end{cases} \tag{5}$$

for each $p = 1(1)n$. It is possible to express (5) as a $N \times N$ linear system of equations

$$G^{(p)} V^{(p)} = F^{(p)} \quad \text{for } p = 1(1)n,$$

where $V^{(p)} = [V_1^{(p)}, V_2^{(p)}, \ldots, V_N^{(p)}]$, $F^{(p)} = [F_1^{(p)}, F_2^{(p)}, \ldots, F_N^{(p)}]$, $\mu_p = \dfrac{h^{-\alpha_p}}{\Gamma(2-\alpha_p)}$, and for $i = 1(1)N$

$$\begin{cases} G_{i,i}^{(p)} = \mu_p b_1^{(p)} + a_{ii}(t_j), \\ G_{i,k}^{(p)} = a_{ik}(t_j), \quad k = i+1(1)n, \\ G_{l,i}^{(j)} = a_{il}(t_j), \quad l = 1(1)i-1, \\ F_i^{(j)} = f_j^{(i)} + \mu b_1^{(p)} V_{j-1}^{(i)} + \displaystyle\sum_{k=0}^{j-2} \left(V_k^{(i)} - V_{k+1}^{(i)}\right) b_{j-k}^{(p)}. \end{cases}$$

4 Convergence analysis

This section establishes the convergence result and estimates the global error of the proposed scheme (3).

Lemma 1. *Truncation error of the discretization from (3) satisfies*

$$|\varepsilon_j^{(p)}| \le C\tau^{2-\alpha_p}, \quad j = 1(1)N.$$

Proof. Let $v^{(p)}(t) \in \mathscr{C}^2[0,T]$, we have

$$\begin{aligned} |\varepsilon_j^{(p)}| &= \left|(\mathscr{D}_t^{\alpha_p} - \mathscr{D}_N^{\alpha_p}) v^p(t_j)\right| \\ &= \left| \frac{1}{\Gamma(1-\alpha_p)} \sum_{k=0}^{j-1} \int_{t_k}^{t_{k+1}} (t_j - s)^{-\alpha_p} \left[\frac{dv^{(p)}(s)}{ds} - \frac{v^{(p)}(t_{k+1}) - v^{(p)}(t_k)}{\tau} \right] ds \right| \\ &\le C \left| \frac{1}{\Gamma(1-\alpha_p)} \sum_{k=0}^{j-1} \int_{t_k}^{t_{k+1}} \frac{t_j + t_{j-1} - 2s}{(t_j - s)^{\alpha_p}} ds + O(\tau^2) \right|. \end{aligned}$$

From [13], we get $\left| \dfrac{1}{\Gamma(1-\alpha_p)} \displaystyle\sum_{k=0}^{j-1} \int_{t_k}^{t_{k+1}} \frac{t_j + t_{j-1} - 2s}{(t_j - s)^{\alpha_p}} ds \right| \le 2\tau^{2-\alpha_p}$. This however means $|\varepsilon_j^{(p)}| \le C\tau^{2-\alpha_p}$. Hence the proof is completed. □

Denote $e_j^{(p)} = \left|v^{(p)}(t_j) - V_j^{(p)}\right|$ for $j = 1(1)N$. From (4) and (5), we get

$$\begin{cases} \mathscr{D}_N^{\alpha} e_j^{(p)} + \sum_{i=1}^{n} a_{pi}(t_j)\, e_j^{(i)} = \varepsilon_j^{(p)}, \\ e_0^{(p)} = 0. \end{cases} \tag{6}$$

Lemma 2. *For any mesh function* $\{V_j^{(p)}\}_{j=0}^{N}$ *with* $V_0^{(p)} = 0$, *we have for* $j = 1(1)N$,

$$\left|V_j^{(p)}\right| \le \max_{k=1(1)j} \left\{ \frac{\Gamma(2-\alpha_p)}{b_k^{(p)} \tau^{-\alpha_p}} \mathscr{D}_N^{\alpha_p} \left|V_k^{(p)}\right| \right\}.$$

Proof. Let $\max\limits_{k=1(1)j} \left|V_k^{(p)}\right| = \left|V_q^{(p)}\right|$ for some $q \in \{1, 2, \cdots, j\}$. Since $V_0^{(p)} = 0$, (3) yields

$$\mathscr{D}_N^{\alpha} \left|V_q^{(p)}\right| = \frac{\tau^{-\alpha_p}}{\Gamma(2-\alpha_p)} \left\{ \left|V_q^{(p)}\right| - \sum_{k=1}^{q-1} \left(b_k^{(p)} - b_{k+1}^{(p)}\right) \left|V_{q-k}^{(p)}\right| \right\}.$$

Now, $b_1^{(p)} = 1$ and $b_k^{(p)} > b_{k+1}^{(p)}$ for all $k \ge 1$ implies that

$$\mathscr{D}_N^{\alpha} \left|V_q^{(p)}\right| \ge \frac{\tau^{-\alpha_p}}{\Gamma(2-\alpha_p)} \left\{ \left|V_q^{(p)}\right| - \sum_{k=1}^{q-1} \left(b_k^{(p)} - b_{k+1}^{(p)}\right) \left|V_q^{(p)}\right| \right\} \ge \frac{\tau^{-\alpha_p}}{\Gamma(2-\alpha)} b_q^{(p)} \left|V_q^{(p)}\right|.$$

Therefore, $\left|V_q^{(p)}\right| \le \dfrac{\Gamma(2-\alpha_p)}{b_q^{(p)} \tau^{-\alpha_p}} \mathscr{D}_N^{\alpha_p} \left|V_q^{(p)}\right|$. Hence, the desired result. □

Theorem 1. *Let* $\{v^{(p)}(t_j)\}_{j=1}^{N}$ *be the true solution and* $\{V_j^{(p)}\}_{j=1}^{N}$ *be the approximate solution of problem (2) for each* $p = 1(1)n$. *Then we have*

$$\left|e_j^{(p)}\right| \le C T^{\alpha_p} (\tau^{\min\limits_{p}\{2-\alpha_p\}} + T\tau^2).$$

Proof. Multiplying (6) by $e_j^{(p)}$ and using (3), we obtain

$$\mu \left|e_j^{(p)}\right|^2 + \sum_{i=1}^{n} \left|a_{pi}(t_j)\right| \left|e_j^{(i)}\right| \left|e_j^{(p)}\right| \le \left|\left|e_j^{(p)}\right| + \mu \sum_{k=1}^{j-1} \left(b_k^{(p)} - b_{k+1}^{(p)}\right) \left|e_{j-k}^{(p)}\right| \left|e_j^{(p)}\right|.$$

Therefore

$$\mu \left|e_j^{(p)}\right|^2 \le \left|e_j^{(p)}\right| + \mu \sum_{k=1}^{j-1} \left(b_k^{(p)} - b_{k+1}^{(p)}\right) \left|e_{j-k}^{(p)}\right| \left|e_j^{(p)}\right|.$$

Dividing by $\left|e_j^{(p)}\right|$, we get $\mathscr{D}_N^{\alpha} \left|e_j^{(p)}\right| \le \left|\mathscr{E}_j^{(p)}\right|$. Lemma 1 shows that

$$\left|\mathscr{E}_j^{(p)}\right| \le \left|\varepsilon_j^{(p)}\right| \le C(\tau^{\min\limits_{p}\{2-\alpha_p\}} + T\tau^2) \quad \text{if} \quad v^{(p)}(t) \in \mathscr{C}^2[0,T].$$

Since $b_1^{(p)} = 1$ and $b_q^{(p)} > b_{q+1}^{(p)}$ for all $q \geq 1$, the mean value theorem implies that

$$(1-\alpha_p)q^{-\alpha_p} \leq b_q^{(p)} \leq (1-\alpha_p)(q-1)^{-\alpha_p} \text{ for } q \geq 2,$$

and using Lemma 2, we obtain

$$\begin{aligned}
\left|e_j^{(p)}\right| &\leq \max_{k=1,2,\ldots,j} \left\{ \frac{\tau^{\alpha_p}\Gamma(2-\alpha_p)}{b_k^{(p)}} \left|\mathscr{E}_j^{(p)}\right| \right\} \\
&\leq \frac{\tau^{\alpha_p}\Gamma(2-\alpha_p)}{(1-\alpha_p)N^{-\alpha_p}} C(\tau^{\min_p\{2-\alpha_p\}} + T\tau^2) \\
&\leq CT^{\alpha_p}\left(\tau^{\min_p\{2-\alpha_p\}} + T\tau^2\right).
\end{aligned}$$

This proves the theorem. □

5 Numerical illustration

To demonstrate the effectiveness of the proposed approach, we present a couple of test examples in this section. By comparing the results for various fractional orders, we establish that the proposed method is highly effective and convenient. The maximum error (Σ_N) and the corresponding order of convergence (ρ_N) are calculated by

$$\Sigma_N = \max_{0\leq j\leq N} \left|V(t_j) - V_j\right|, \quad \rho_N = \log_2\left(\Sigma_N/\Sigma_{2N}\right). \tag{7}$$

Numerical computations are performed in MATLAB R2016a.

Example 1. Consider the following test case in $t \in (0,1]$:

$$\begin{cases}
\mathscr{D}_t^{\alpha_1} v^1(t) + v^1(t) + v^2(t) = g_1(t), \\
\mathscr{D}_t^{\alpha_2} v^2(t) + v^1(t) + v^2(t) = g_2(t), \\
v^1(0) = v^2(0) = 0.
\end{cases}$$

We choose $g_1(t)$ and $g_2(t)$ so that the exact solution becomes $v^1(t) = t^{(2+\alpha_1+\alpha_2)}$, $v^2(t) = -t^{(3+\alpha_1+\alpha_2)}$. Figure 1 depicts the comparison between the exact and approximate solutions for Example 1 with varying values of α_1 and fixed $\alpha_2 = 0.5$. Similarly, Figure 2 shows the approximate solutions of $v^1(t)$ and $v^2(t)$ for fixed $\alpha_2 = 0.5$ and varying α_1 . It is clear from the graphs that the approximate solutions get closer to the exact one. Figures 3-4 illustrate the effect of fractional order on the solutions profile for $v^1(t)$ and $v^2(t)$, respectively and confirm the stability and accuracy of the proposed method. Numerical computations of Σ_N and ρ_N in Table 1 demonstrate that the proposed scheme achieves convergence rates ranging from approximately 1.10 to 1.49 for $v^1(t)$, depending on the chosen fractional orders. A similar trend is observed for $v^2(t)$ in Table 2, with convergence rates ranging from 1.16 to 1.49. It can be observed that the order of convergence increases with increasing values of α_1 and α_2, in agreement with the theoretical estimate of $\mathscr{O}(\tau^{2-\alpha_p})$ for the proposed scheme. Figures 5 present the log-log plots of the error versus the number of discretization points N for different values of α_1 and α_2, respectively. The observed slopes align well with the theoretical convergence rates, validating the accuracy of the proposed scheme.

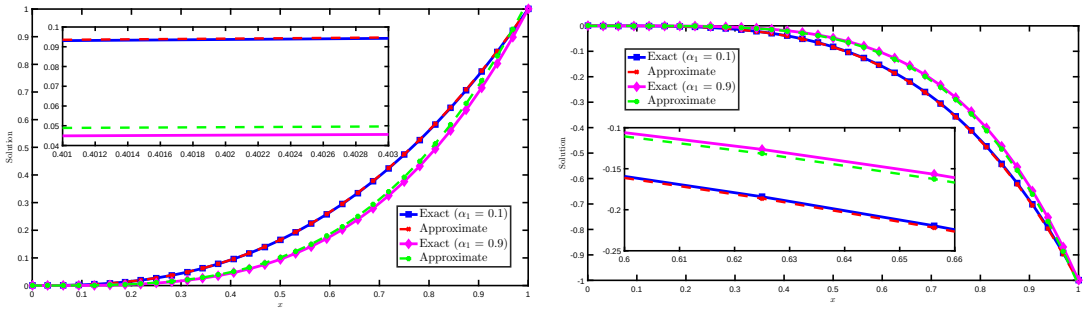

(a) $v^1(t)$ **(b)** $v^2(t)$

Figure 1: The exact and approximate solutions with $\alpha_2 = 0.5$, $N = 32$ for Example 1

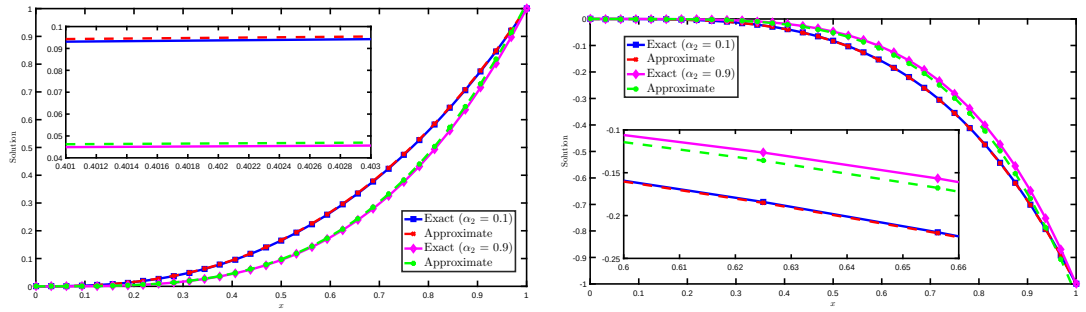

(a) $v^1(t)$ **(b)** $v^2(t)$

Figure 2: The exact and approximate solutions with $\alpha_1 = 0.5$, $N = 32$ for Example 1

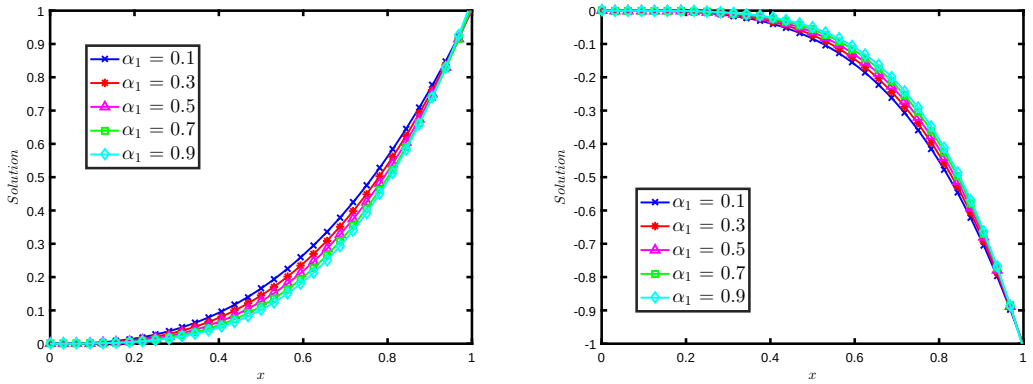

(a) $v^1(t)$ **(b)** $v^2(t)$

Figure 3: The approximate solutions with $\alpha_2 = 0.5$, $N = 32$ for Example 1

Figures 6 show the surface plots of the numerical error with respect to the fractional orders α_1, α_2, and the mesh size N. The decreasing trend of the error across the domain demonstrates the stability and effectiveness of the proposed numerical method.

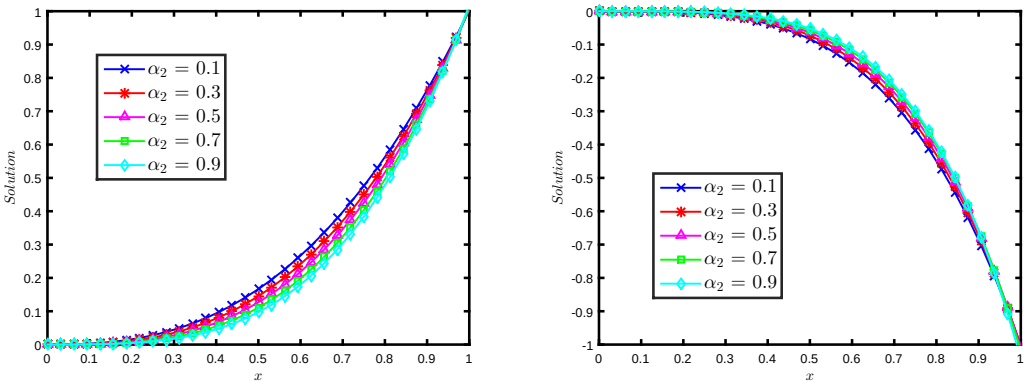

(a) $v^1(t)$ **(b)** $v^2(t)$

Figure 4: The approximate solutions with $\alpha_1 = 0.5$, $N = 32$ for Example 1

Table 1: Σ_N *and* ρ_N *of* v^1 *for Example 1*

(α_1, α_2)	32	64	128	256	512	1024
(0.1,0.9)	1.774E-2	8.276E-3	3.861E-3	1.802E-3	8.405E-4	3.921E-4
	1.100	1.100	1.100	1.100	1.100	1.100
(0.2,0.8)	1.140E-2	4.945E-3	2.145E-3	9.307E-4	4.040E-4	1.755E-4
	1.205	1.205	1.205	1.204	1.203	1.202
(0.3,0.7)	7.735E-3	3.097E-3	1.239E-3	4.957E-4	1.987E-4	7.977E-5
	1.321	1.322	1.321	1.319	1.316	1.314
(0.4,0.6)	6.050E-3	2.255E-3	8.350E-4	3.083E-4	1.137E-4	4.196E-5
	1.424	1.433	1.437	1.439	1.438	1.437
(0.5,0.5)	6.003E-3	2.189E-3	7.908E-4	2.837E-4	1.013E-4	3.608E-5
	1.455	1.469	1.479	1.485	1.490	1.493
(0.6,0.4)	7.557E-3	2.873E-3	1.085E-3	4.083E-4	1.534E-4	5.757E-5
	1.395	1.405	1.410	1.413	1.414	1.414
(0.7,0.3)	1.097E-2	4.467E-3	1.812E-3	7.341E-4	2.972E-4	1.203E-4
	1.296	1.301	1.304	1.305	1.305	1.304
(0.8,0.2)	1.681E-2	7.349E-3	3.205E-3	1.396E-3	6.077E-4	2.645E-4
	1.194	1.197	1.199	1.200	1.200	1.200
(0.9 ,0.1)	2.602E-2	1.218E-2	5.691E-3	2.658E-3	1.240E-3	5.789E-4
	1.096	1.097	1.099	1.099	1.100	1.100

Example 2. Consider the following model for $t \in (0,1]$:

$$\begin{cases} \mathscr{D}_t^{\alpha_1} v^{(1)}(t) + (1-t)v^{(3)}(t) = f^{(1)}(t), \\ \mathscr{D}_t^{\alpha_2} v^{(2)}(t) + tv^{(1)}(t) = f^{(2)}(t), \\ \mathscr{D}_t^{\alpha_3} v^{(3)}(t) + t^2 v^{(2)}(t) = f^{(3)}(t), \\ v^{(1)}(0) = 0, v^{(2)}(0) = 1, v^{(3)}(0) = 0. \end{cases}$$

To ensure that the exact solution is $v^{(1)}(t) = t(t-1)$, $v^{(2)}(t) = e^t$, $v^{(3)}(t) = t^3$, we choose the source terms $f^{(1)}(t), f^{(2)}(t), f^{(3)}(t)$, accordingly. Figure 7 illustrates the comparison between the exact and

Table 2: Σ_N *and* ρ_N *of* v^2 *with* $\alpha_1 = 0.5$ *for Example 1*

α_2	32	64	128	256	512	1024
0.1	1.815E-3	6.367E-4	2.225E-4	7.765E-5	2.711E-5	9.475E-6
	1.512	1.517	1.519	1.518	1.517	1.515
0.2	2.424E-3	8.333E-4	2.850E-4	9.731E-5	3.325E-5	1.138E-5
	1.541	1.548	1.550	1.549	1.547	1.543
0.3	3.424E-3	1.176E-3	4.006E-4	1.358E-4	4.591E-5	1.552E-5
	1.541	1.554	1.561	1.564	1.565	1.564
0.4	5.052E-3	1.775E-3	6.165E-4	2.126E-4	7.293E-5	2.495E-5
	1.509	1.526	1.536	1.543	1.548	1.550
0.5	7.662E-3	2.805E-3	1.015E-3	3.649E-4	1.304E-4	4.648E-5
	1.450	1.466	1.477	1.484	1.489	1.492
0.6	1.177E-2	4.544E-3	1.739E-3	6.617E-4	2.508E-4	9.488E-5
	1.372	1.386	1.394	1.399	1.403	1.405
0.7	1.809E-2	7.420E-3	3.025E-3	1.228E-3	4.976E-4	2.014E-4
	1.285	1.295	1.300	1.303	1.305	1.306
0.8	2.763E-2	1.207E-2	5.258E-3	2.285E-3	9.922E-4	4.307E-4
	1.195	1.199	1.202	1.204	1.204	1.204
0.9	4.181E-2	1.946E-2	9.056E-3	4.214E-3	1.962E-3	9.133E-4
	1.103	1.104	1.104	1.103	1.103	1.102

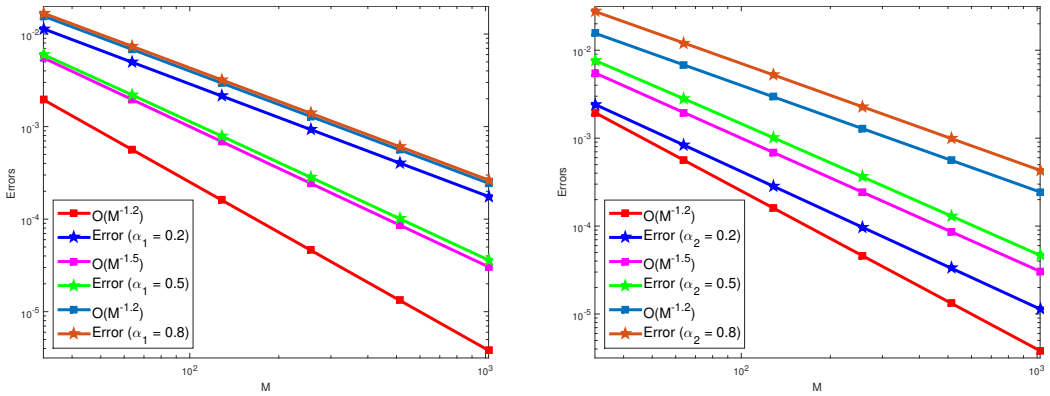

(a) $v^1(t)$ with $\alpha_2 = 1 - \alpha_1$ **(b)** $v^2(t)$ with $\alpha_1 = 0.5$

Figure 5: Log-log plots for Example 1

approximate solutions of $v^{(1)}(t), v^{(2)}(t)$, and $v^{(3)}(t)$ for the parameter values $\alpha_1 = 0.3$, $\alpha_2 = 0.5$, $\alpha_3 = 0.3$. As shown, the numerical solutions obtained using the proposed scheme closely track the exact solutions across the entire domain. Tables 3–5 present the numerical errors Σ_N and the corresponding convergence rates ρ_N for $v^{(1)}$, $v^{(2)}$, and $v^{(3)}$, respectively, under various fractional orders α_i. The results confirm that the proposed method achieves convergence rates ranging from approximately 1.05 to 1.75. As expected, the convergence rate improves with increasing values of the fractional orders, aligning well with the theoretical rate of $\mathscr{O}(\tau^{2-\alpha_i})$. A sharp convergence rate is presented through the log-log plots in Figure 8. Moreover, the surface plots in Figure 9 depict how the error varies with respect to α_i and mesh size N. These plots provide further evidence that the method is robust and performs reliably across a wide range of fractional orders.

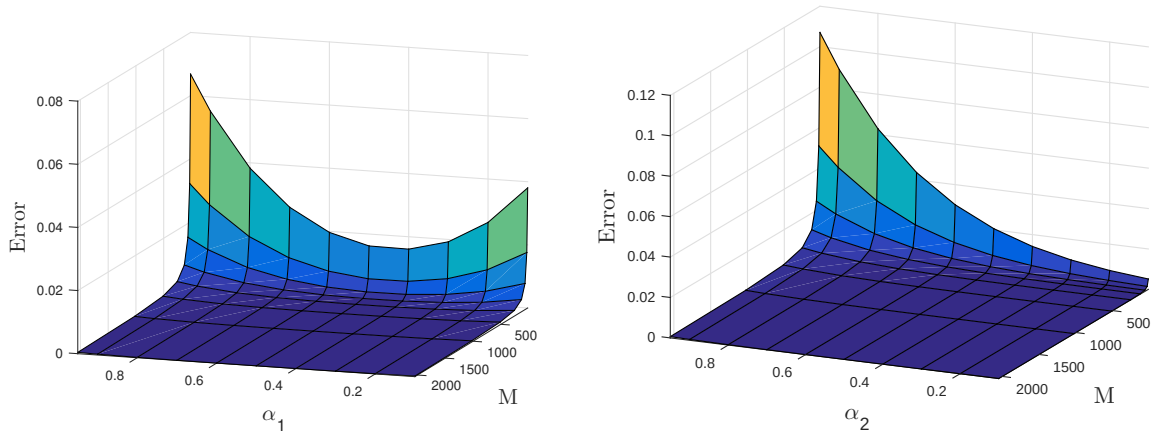

(a) $v^1(t)$ **(b)** $v^2(t)$

Figure 6: Error surface plots for Example 1

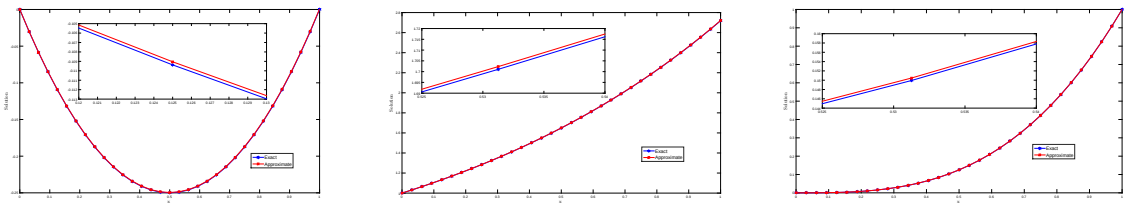

(a) $v^1(t)$ **(b)** $v^2(t)$ **(c)** $v^3(t)$

Figure 7: The exact and approximate solutions with $\alpha_1 = 0.3, \alpha_2 = 0.5, \alpha_3 = 0.3, N = 32$ for Example 2

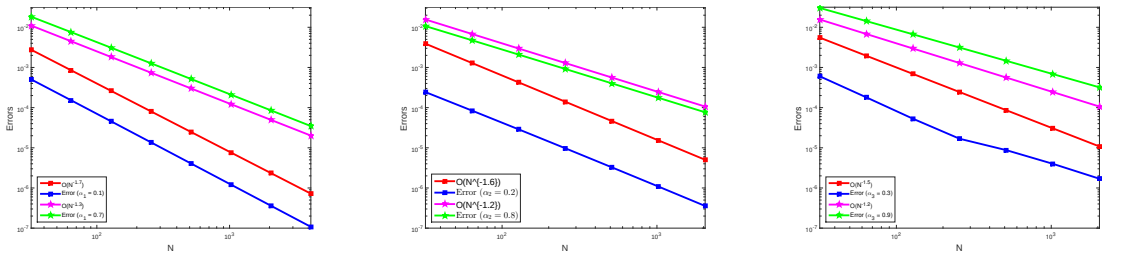

(a) $v^1(t)$ with $\alpha_2 = 0.3, \alpha_3 = 0.1$ **(b)** $v^2(t)$ with $\alpha_1 = 0.4, \alpha_3 = 0.9$ **(c)** $v^3(t)$ with $\alpha_1 = 0.5, \alpha_2 = 0.7$

Figure 8: Log-log plots for Example 2

6 Conclusion

In this work, we have investigated a system of differential equations involving a fractional derivative of distinct orders. To solve this system numerically, the L1 scheme is employed for the differential operators. A thorough convergence analysis was conducted, and it is shown that the numerical method achieves an order of convergence of $(2-\alpha_p)$, where α_p denotes the maximum fractional order among the

Table 3: Σ_N *and* ρ_N *of* $v^{(1)}$ *with* $\alpha_2 = 0.3,\ \alpha_3 = 0.1$ *for Example 2*

α_1	16	32	64	128	256	512	1024
0.10	5.043E-4	1.523E-4	4.567E-5	1.365E-5	4.070E-6	1.213E-6	3.614E-7
	1.728	1.737	1.743	1.745	1.747	1.747	1.746
0.20	1.264E-3	3.893E-4	1.185E-4	3.581E-5	1.077E-5	3.226E-6	9.638E-7
	1.700	1.716	1.727	1.733	1.739	1.743	1.747
0.30	2.497E-3	8.086E-4	2.590E-4	8.231E-5	2.599E-5	8.170E-6	2.558E-6
	1.626	1.642	1.654	1.663	1.670	1.675	1.680
0.40	4.417E-3	1.513E-3	5.132E-4	1.728E-4	5.788E-5	1.932E-5	6.427E-6
	1.546	1.560	1.570	1.578	1.583	1.588	1.591
0.50	7.359E-3	2.677E-3	9.649E-4	3.457E-4	1.234E-4	4.390E-5	1.559E-5
	1.459	1.472	1.481	1.487	1.491	1.494	1.496
0.60	1.178E-2	4.563E-3	1.753E-3	6.703E-4	2.555E-4	9.715E-5	3.690E-5
	1.369	1.380	1.387	1.392	1.395	1.397	1.398
0.70	1.833E-2	7.569E-3	3.105E-3	1.269E-3	5.171E-4	2.105E-4	8.558E-5
	1.276	1.286	1.291	1.295	1.297	1.298	1.299
0.80	2.788E-2	1.228E-2	5.383E-3	2.352E-3	1.026E-3	4.473E-4	1.948E-4
	1.183	1.190	1.194	1.197	1.198	1.199	1.199
0.90	4.165E-2	1.956E-2	9.161E-3	4.283E-3	2.001E-3	9.340E-4	4.359E-4
	1.090	1.094	1.097	1.098	1.099	1.099	1.100
0.95	5.062E-2	2.454E-2	1.188E-2	5.743E-3	2.776E-3	1.341E-3	6.478E-4
	1.045	1.047	1.048	1.049	1.049	1.050	1.050

Table 4: Σ_N *and* ρ_N *of* $v^{(2)}$ *with* $\alpha_1 = 0.3, \alpha_3 = 0.1$ *for Example 2*

α_2	16	32	64	128	256	512	1024
0.10	1.677E-3	5.566E-4	1.828E-4	5.944E-5	1.918E-5	6.149E-6	1.960E-6
	1.591	1.607	1.620	1.632	1.641	1.649	1.656
0.20	6.986E-4	2.435E-4	8.414E-5	2.877E-5	9.731E-6	3.259E-6	1.082E-6
	1.521	1.533	1.548	1.564	1.578	1.591	1.602
0.30	7.914E-4	2.629E-4	8.538E-5	2.733E-5	8.663E-6	2.726E-6	8.534E-7
	1.590	1.622	1.643	1.658	1.668	1.676	1.681
0.40	2.705E-3	9.737E-4	3.438E-4	1.198E-4	4.136E-5	1.418E-5	4.838E-6
	1.474	1.502	1.521	1.534	1.544	1.552	1.558
0.50	5.595E-3	2.120E-3	7.896E-4	2.907E-4	1.062E-4	3.854E-5	1.392E-5
	1.400	1.425	1.441	1.453	1.462	1.469	1.474
0.60	9.737E-3	3.889E-3	1.531E-3	5.966E-4	2.309E-4	8.895E-5	3.413E-5
	1.324	1.345	1.359	1.369	1.376	1.382	1.386
0.70	1.563E-2	6.598E-3	2.752E-3	1.139E-3	4.689E-4	1.923E-4	7.864E-5
	1.245	1.261	1.273	1.281	1.286	1.290	1.293
0.80	2.397E-2	1.071E-2	4.745E-3	2.090E-3	9.173E-4	4.015E-4	1.754E-4
	1.162	1.174	1.183	1.188	1.192	1.195	1.196
0.90	3.570E-2	1.689E-2	7.959E-3	3.738E-3	1.751E-3	8.194E-4	3.830E-4
	1.079	1.086	1.090	1.094	1.096	1.097	1.098
0.95	4.322E-2	2.105E-2	1.023E-2	4.961E-3	2.403E-3	1.163E-3	5.622E-4
	1.038	1.041	1.044	1.046	1.047	1.048	1.049

system components. This theoretical establishment was further validated through numerical experiments. Future work will focus on refining the method using graded temporal meshes to better handle initial

Table 5: Σ_N *and* ρ_N *of* $v^{(3)}$ *with* $\alpha_1 = 0.3$, $\alpha_2 = 0.5$ *for Example 2*

α_3	16	32	64	128	256	512	1024
0.10	3.787E-3	1.524E-3	5.941E-4	2.266E-4	8.500E-5	3.150E-5	1.157E-5
	1.314	1.359	1.391	1.414	1.432	1.446	1.456
0.20	1.615E-3	7.898E-4	3.497E-4	1.457E-4	5.837E-5	2.273E-5	8.674E-6
	1.032	1.176	1.263	1.320	1.361	1.390	1.412
0.30	1.981E-3	6.029E-4	1.799E-4	5.290E-5	1.680E-5	8.750E-6	3.994E-6
	1.717	1.745	1.766	1.655	0.941	1.131	1.234
0.40	5.335E-3	1.757E-3	5.705E-4	1.836E-4	5.874E-5	1.871E-5	5.937E-6
	1.603	1.623	1.636	1.644	1.651	1.656	1.660
0.50	1.091E-2	3.996E-3	1.444E-3	5.172E-4	1.842E-4	6.538E-5	2.315E-5
	1.448	1.469	1.481	1.489	1.495	1.498	1.500
0.60	1.864E-2	7.331E-3	2.851E-3	1.100E-3	4.228E-4	1.620E-4	6.194E-5
	1.346	1.363	1.373	1.380	1.384	1.387	1.389
0.70	2.934E-2	1.228E-2	5.095E-3	2.101E-3	8.630E-4	3.536E-4	1.446E-4
	1.256	1.269	1.278	1.284	1.287	1.290	1.292
0.80	4.411E-2	1.959E-2	8.654E-3	3.806E-3	1.669E-3	7.307E-4	3.194E-4
	1.171	1.179	1.185	1.189	1.192	1.194	1.195
0.90	6.442E-2	3.032E-2	1.425E-2	6.683E-3	3.130E-3	1.465E-3	6.848E-4
	1.087	1.090	1.092	1.094	1.096	1.097	1.098
0.95	7.728E-2	3.742E-2	1.813E-2	8.781E-3	4.251E-3	2.057E-3	9.948E-4
	1.046	1.045	1.046	1.047	1.047	1.048	1.048

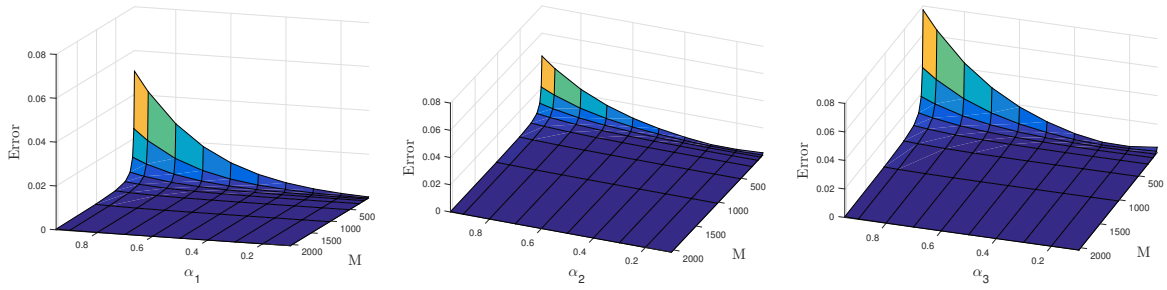

(a) $v^1(t)$ **(b)** $v^2(t)$ **(c)** $v^3(t)$

Figure 9: Error surface plots for Example 2

singularities and on extending the approach to multi-scale or real-world models involving fractional-order dynamics.

Conflicts of interest

The authors declare that there are no conflicts of interest.

References

[1] T. Abdeljawad, R. Amin, K. Shah, Q. Al-Mdallal, F. Jarad, *Efficient sustainable algorithm for numerical solutions of systems of fractional order differential equations by Haar wavelet collocation method*, Alex. Eng. J. **59(4)** (2020) 2391–2400.

[2] S.A. T. Algazaa, J. Saeidian, *Solving nonlinear multi-order fractional differential equations using Bernstein polynomials*, IEEE Access **11** (2023) 128032–128043.

[3] F. Chen, Q. Xu, J. S. Hesthaven, *A multi-domain spectral method for time-fractional differential equations*, J. Comput. Phys. **293** (2015) 157–172.

[4] D. Delbosco, L. Rodino, *Existence and uniqueness for a nonlinear fractional differential equation*, J. Math. Anal. Appl. **204(2)** (1996) 609–621.

[5] K. Diethelm, S. Siegmund, H.T. Tuan, *Asymptotic behavior of solutions of linear multi-order fractional differential systems*, Fract. Calc. Appl. Anal. **20(5)** (2017) 1165–1195.

[6] B. Duan, Z. Zheng, W. Cao, *Spectral approximation methods and error estimates for Caputo fractional derivative with applications to initial-value problems*, J. Comput. Phys. **319** (2016) 108–128.

[7] B. Ghosh, J. Mohapatra, *Numerical simulation for two species time fractional weakly singular model arising in population dynamics*, Int. J. Model. Simul. **45(4)** (2023) 1383–1396.

[8] M.M. Khader, T.S El Danaf, A.S. Hendy, *A computational matrix method for solving systems of high order fractional differential equations*, Appl. Math. Model. **37(6)** (2013) 4035–4050.

[9] R. Khalil, M. Al Horani, A. Yousef, M. Sababheh, *A new definition of fractional derivative*, J. Comput. Appl. Math. **264** (2014) 65–70.

[10] A.A. Kilbas, *Theory and Applications of Fractional Differential Equations*, North-Holland Mathematics Studies, New York, 2006.

[11] M.E. Koksal, M. Senol, A. K Unver, *Numerical simulation of power transmission lines*, Chin. J. Phys. **59** (2019) 507–524.

[12] D. Kumar, J. Singh, D. Baleanu, *On the analysis of vibration equation involving a fractional derivative with Mittag-Leffler law*, Math. Methods Appl. Sci. **43(1)** (2020) 443–457.

[13] Y. Lin, C. Xu, *Finite difference/spectral approximations for the time-fractional diffusion equation*, J. Comput. Phys. **225(2)** (2007) 1533–1552.

[14] F. Mainardi, *Fractional calculus: some basic problems in continuum and statistical mechanics*, Fractals and Fractional Calculus in Continuum Mechanics (1997) 291–348.

[15] J. Mohapatra, S.P. Mohapatra, A. Nath, *An approximation technique for a system of time-fractional differential equations arising in population dynamics*, J. Math. Model. **13(3)** (2025) 519–531.

[16] J. Mohapatra, *Equidistribution grids for two-parameter convection–diffusion boundary-value problems*, J. Math. Model. **2(1)** (2014) 1–21.

[17] Z.M. Odibat, *Analytic study on linear systems of fractional differential equations*, Comput. Math. Appl. **59(3)** (2010) 1171–1183.

[18] I. Podlubny, *Fractional Differential Equations, Mathematics in Science and Engineering*, Academic press, New York, 1999.

[19] U. Ruman, M.S. Islam, *Numerical solutions of linear fractional order BVP by Galerkin residual method with differentiable polynomials*, Appl. Math. Comput. **9(2)** (2020) 20–25.

[20] G. Saini, B. Ghosh, S. Chand, J. Mohapatra, *An iterative-based difference scheme for nonlinear fractional integro-differential equations of Volterra type*, Partial Differ. Equ. Appl. Math. **13** (2025) 101138.

[21] M. Senol, O. Tasbozan, A. Kurt, *Comparison of two reliable methods to solve fractional Rosenau-Hyman equation*, Math. Meth. Appl. Sci. **44(10)** (2021) 7904–7914.

[22] S. Soradi-Zeid, *Efficient radial basis functions approaches for solving a class of fractional optimal control problems*, Comput. Appl. Math. **39(1)** (2020) 20.

[23] P. Veeresha, L. Akinyemi, K. Oluwasegun, M. Şenol, B. Oduro, *Numerical surfaces of fractional Zika virus model with diffusion effect of mosquito-borne and sexually transmitted disease*, Math. Methods Appl. Sci. **45(5)** (2022) 2994–3013.

[24] M. Zayernouri, G.E. Karniadakis, *Fractional spectral collocation method*, SIAM J. Sci. Comput. **36(1)** (2014) A40–A62.

[25] D. Ziane, M.H. Cherif, *Variational iteration transform method for fractional differential equations*, J. Interdiscip. Math. **21(1)** (2018) 185–199.